Experimental investigation of plasma assisted combustion of low Heating Value biomass with a three phase AC plasma torch

Sabri Takali, Frédéric Fabry, Vandad-Julien Rohani, François Cauneau, Laurent Fulcheri

Experimental investigation of plasma assisted combustion of low Heating Value biomass with a three phase AC plasma torch

S. Takali, F. Fabry, V. Rohani, F. Cauneau and L. Fulcheri

MINES ParisTech, PSL-Research University, PERSEE Centre for processes, renewable energy and energy systems, rue Claude Daunesse, CS 10207, 06904 Sophia Antipolis Cedex, France, Phone:+33.493.957.540.
E-mail: sabri.takali@mines-paristech.fr.

Abstract. A wide array of applications exist for mid-range power plasma torches (tens of kW) starting from municipal waste gasification to the synthesis of chemical products. The majority of commercialized plasma torches are working in inert or reductive environments. Recent feasibility study demonstrated the economic profitability of the plasma assisted combustion for the start-up of coal and biomass thermal power plants. In order to prove the technical feasibility of this application, a three phase plasma torch working with consumable graphite electrodes and operating with air at 100 kWe, has been developed. Hereafter, the specifications of this plasma torch are detailed along with a briefing on the early CFD simulation and the main technical challenges encountered. A set of experiments are performed to validate the concept and characterize the torch, first, without combustion, and then, with the injection of a biomass sample. Different feeding rates are also tested. First results showed excellent combustion efficiency. Burned gases are analyzed using gas chromatograph and non-dispersive infrared sensor. In addition, a high speed camera (up to 1 million fps) showed particle behavior inside the plasma and graphite electrode erosion process. The overall results confirmed the technical feasibility of the plasma assisted combustion for the tested sample and the reliability of the developed three phase plasma torch.

1. Introduction

Plasma as the fourth state of matter provides fast thermal heating (the Joule effect), high electron energy (1-100 eV) in addition to electromagnetic forces [1]. Thus, plasma can enhance combustion of lean mixture in different ways. First, trough thermal effect, by rapidly increasing gas temperature thanks to energy transfer from charged particles to neutral molecules, it accelerates the chemical reaction governed by the Arrhenius law. Second, thanks to the high amount of produced radicals especially atomic oxygen and hydroxyl, fuel chains are easily cracked and exothermal molecule formation are rapidly produced. Plasma has also a mixing effect nearby the arc discharge due to the repulsive Lorentz forces which increases the residence time for combustible particle passing through and implies better energy yielding.

Plasma assisted combustion have great potential at small power scale (car engines [1]–[3]), medium power scale (jet engines and gas turbines [4], [5]), and even big power scale (power plant thermal furnaces [6]–[10]). In the case of thermal power plants, the economic and ecologic issues faced within combustion are as important as the impact of this energy sector. Economically, the increasing flexibility demand on coal and biomass power plants, for competitiveness reasons, is pushing the furnace operation for more frequent startups or at least low load firing. Almost all European thermal power plants use heavy oil for startup burners which induces higher operating expenses and implies more pollutant emissions due to the disabling of filters during startup phase. With the actual burners, two main challenges face the use of alternative poor heating value combustible like biomass: combustion ignition and hazardous emissions. Since plasma is known for enlarging the flammability limits and reducing NOx emissions, it is potentially a promising option for a breakthrough in the old and conservative large scale burner industry. Different type of plasma are implemented and used for combustion assistance. In this work, the plasma is created by arc discharge between three graphite electrodes connected to a 3 phase AC power source.

A numerical model was developed to simulate the plasma flow inside the torch in order to verify the thermal resistance of the different components of the torch and predict the outlet conditions. This stationary model is based a simplified source volume that represents the arc column and replaces the different electromagnetic phenomena with a source of power -image of energy yielding- and momentum source representing the electromagnetic forces. This assumption is made to reduce calculation costs and allow simulating all the element of the torch including the solid ones: the graphite electrodes, the electric insulation of the electrodes, the thermal insulation ceramic and the stainless steel walls but also the water sheeting that cools the walls. The simulation integrates air radiation via a 6 band mean absorption coefficient developed recently through a detailed model that takes into account 30 different species. Results show how the radiation redistributes the energy on the gas and the walls and increases thermal losses to the wall. In addition, solid temperatures are predicted to be in the operating range. In Table 1 are resumed the minimum, maximum and average temperature of the different modelled zones of the torch with the wall heat losses. These results are associated to a power of 100 kWe and a gas flow rate of 65 $Nm^3.h^{-1}$.

Table 1: Temperature of the different modeled zones and wall thermal losses (simulation results)

	T max (°K)	T moy (°K)	T max (°K)
Arc zone	4926	8558	10509
Gas	299	690	9564
Water	299	303	344
Steel	299	373	474
Ceramic	980	1187	1420
Electrode	603	978	2138
Wall heat flux	16.590 kW ≈ 16.7 %		

2. Experimental setup

The principal elements of the experimental setup are: the three phase plasma torch, the combustion chamber, the power source, the biomass feeding injector, the cooling system and the measurement setup.

The AC plasma torch is equipped with graphite electrodes and designed to work with air with a flow rate of 55 $Nm^3.h^{-1}$ and with a nitrogen electrode sheeting at 10 $Nm^3.h^{-1}$. For efficiency reasons, a ceramic shield is placed inside the torche to reduce heat losses especially by radiation. A double layer steel wall allows water from the cooling system to keep the wall temperature in the operational range. The cooling system can provide up to 10 $m^3.h^{-1}$ of room temperature water in a closed loop at 6 bar of pressure. The water pipes are connected separately to the different elements which allows the quantification of thermal losses via thermocouples plugged at the inlet and outlet of each circuit as shown in Figure 2.

According to the characteristics of the power supply, the frequency can be the same as the public network, 50 Hz or 60 Hz using a single transformer, up to higher frequencies of several kHz using a more sophisticated power converter. In this study, a 263 kilowatt 3-phase converter (chopper rectifier-inverter) was used and the frequency is set at 80 Hz. The current could be tuned in the range of 150 to 400 A. The feeding power can reach 100 kW at optimal inter-electrodes distance. For this amperage to be not harmful, the electrode diameter is defined at 25 mm. At a constant current, the source electric power is mainly a function of the plasma gas, the gap between electrode tips and the angle between the electrodes. In fact, the arc discharge is characterized with electrode jets that accelerate the gas nearby the cathode and anode spots reaching the speed of several hundreds of $m.s^{-1}$, thus, imposing to the arc roots a perpendicular direction to the electrode tips. Maecker effect is at the origin of this phenomena happening because of the restriction of current section at the interface between the arc and the electrode. For a current set at 400 A, magneto-hydrodynamic simulation predicts electrode jet speed as high as 360 m.s-1 [11]. Hence, the shape of the arc column depends of the angle between the electrodes: if the electrode configuration is planar, the electrode jets are also confined in the same plan and the arc column has a minimum of distortion, while if the electrode configuration is angular, the electrode jets pushes the arc away from the other electrodes which distorts to reach the opposite electrode and assure the current continuity. Thus, in the studied torche electrodes have 20° to the main axis which gives the arc column a longer distance and higher resistance and consequently extracts higher power from the source for the same current value.

The combustion chamber is cylindrical and has a double layer of stainless steel for cooling purposes. It contains multiple circular windows at different high levels and angles and a big rectangular window along the vertical axis giving the possibility to visualize, in addition to the combustion zone, the discharge volume in the torch. This window is made of two 836 by 136 mm borosilicate glasses put in sandwich with a film of cooling water circulating between.

The biomass feeding system is a homemade injector equipped with an endless screw and has a maximum speed of 2 000 rpm associated to a maximum feeding rate 8 $kg.h^{-1}$. The combustible is mixed inside the injector with air and then conducted to the torch via a copper duct in order to avoid any risk of sparkling.

The high speed camera used is an Olympus i-speed FS with an acquisition speed up to 1 million frames per second (fps) with a minimum resolution of 24X8 pixels. Since the current frequency is set to 80 Hz, a speed of 150 000 fps is sufficient to fully describe the behavior of the arc discharge and the combustible particles inside the torch.

Wood ships are selected as test sample. Its heating values, water content, percentages of sulfur, hydrogen and ash are summarized in Table 2 and Figure 1.

Table 2 : Characteristics of the tested biomass (percentages are in mass)

Wood chips		
Raw fuel		
moisture	%	5
Ash content	%	0.29
Net heating value	$MJ.kg^{-1}$	20.51
Density	$Kg.m^{-3}$	300
Ash softening point	°C	1150
Dry ash free fuel		
Volatiles	%	80.00
Dry fuel		
Ash	%	0.50
C	%	49.75
H	%	6.12
N	%	0.05
O	%	43.50
S	%	0.04
Cl	$Mg.kg^{-1}$	100
P	$Mg.kg^{-1}$	100
alkaline (Na + K)	$Mg.kg^{-1}$	600

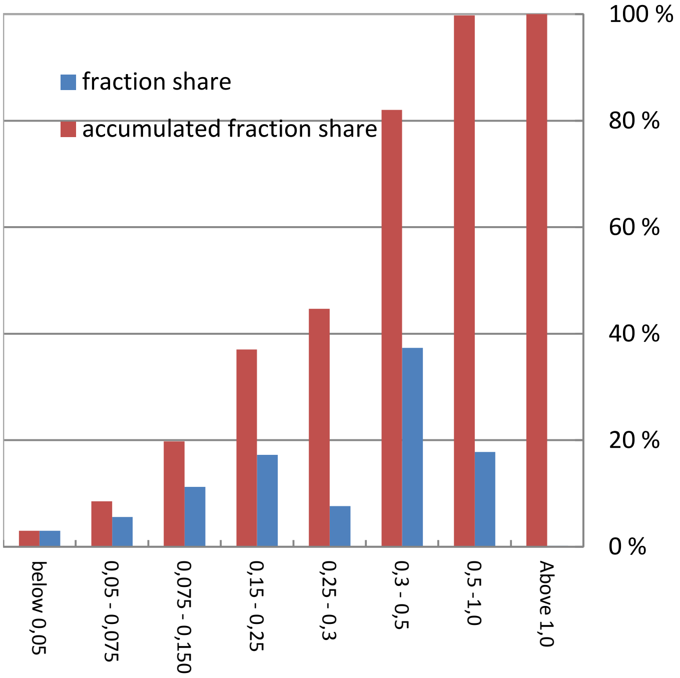

Figure 1: Mass distribution of biomass granulometry (dimension in mm).

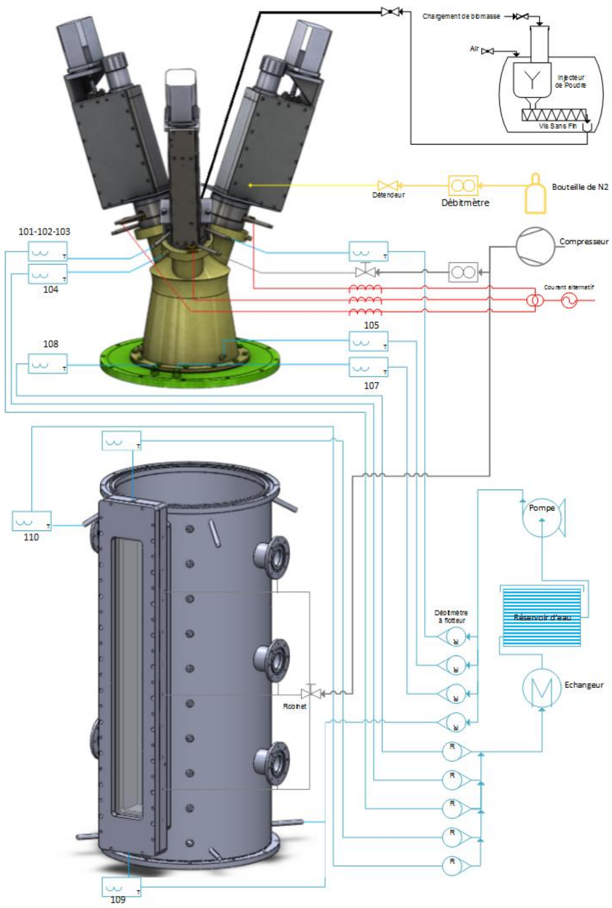

Figure 2 : P&D of the experimental setup (three phase plasma torch (top left) and combustion chamber (bottom left))

The measuring and diagnostic equipment includes a gas chromatograph and a Non-Dispersive InfraRed (NDIR) sensor for outlet gas identification, high speed camera for qualitative analysis and an oscilloscope with the previously mentioned thermocouples for power balance calculations. The gas chromatograph used here is a Perichrom PR2100 equipped with two columns: Porapak Q and Porapak T, both have a stationary phase made of porous polymer, ideal for the detection of organic molecules like CO, CO_2 and CH_4 [12]. The chromatograph has also a Flame Ionization Sensor (FID) and a universal Thermal Conductivity Sensor (TCD). As for the Non-Dispersive InfRared (NDIR) sensor, it is a NDIR-TCD ROSEMOUNT NGA 2000 MLT 4, capable of continuously detecting molar fraction of CO, CO_2, CH_4, and H_2, present in a matrix of nitrogen in the following percentage ranges: $H_2 \in [0, 40]$, $CO \in [0, 24]$, $CO_2 \in [0, 16]$, $CH_4 \in [0, 8]$.

3. Results of the plasma assisted combustion test

Due to the existence of multiple windows on the combustion chamber and the different junction in the system, not all thermal power could be quantified. This explains the gap between total measured heat losses and electric power as shown in Figure 3. After 10 minutes of heating phase, one can notice that non-measured heat losses are almost stabilized and the averaged value is approximately equal to -5.68 kW. As shown in Figure 3, the combustion test is performed in 5 parts: heating phase without combustion, injection of 1.1 $kg.h^{-1}$, then 2.2 $kg.h^{-1}$, then 3.3 $kg.h^{-1}$ and finally a rapid stop and run test. The first four steps last each 15 minutes. The difference between measured thermal power and measured electric power rise during the three successive injection rates to -0.40 kW, 5.09 kW and 11.20 kW. The average power provided by combustion is equal to 5.62 kW/kg which is near to what a total combustion would produce.

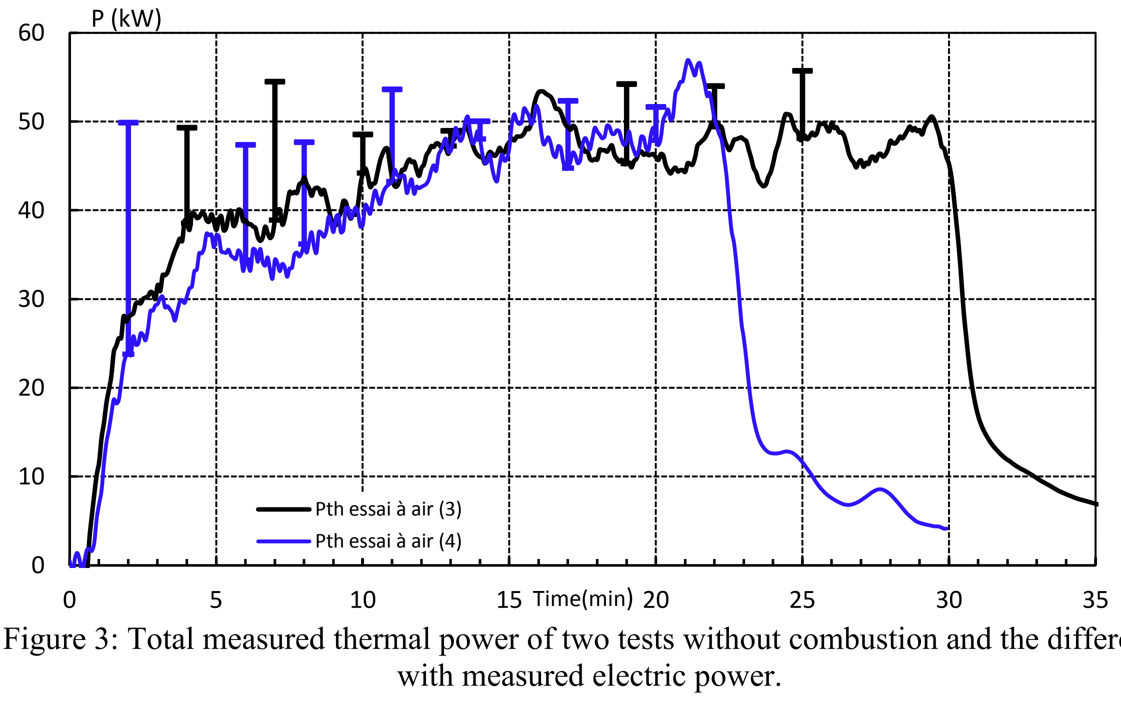

Figure 3: Total measured thermal power of two tests without combustion and the difference with measured electric power.

Burned gas analysis using NDIR sensor, are plotted in Figure 4 at different biomass feeding rates. We notice that CO_2 emissions are proportional to the feeding rate similarly to the combustion power. The CO emissions could be neglected since it represents merely 2% of CO_2 emissions. The amount of hydrogen measured is coherent with the content of the raw biomass. The estimation of combustion efficiency through gas emissions exceeds 95%. The measurement of CO_2 emissions using gas chromatography gives a different value to the NDIR sensor with an average value of 0.51. In our case, the NDIR sensor results are more reliable.

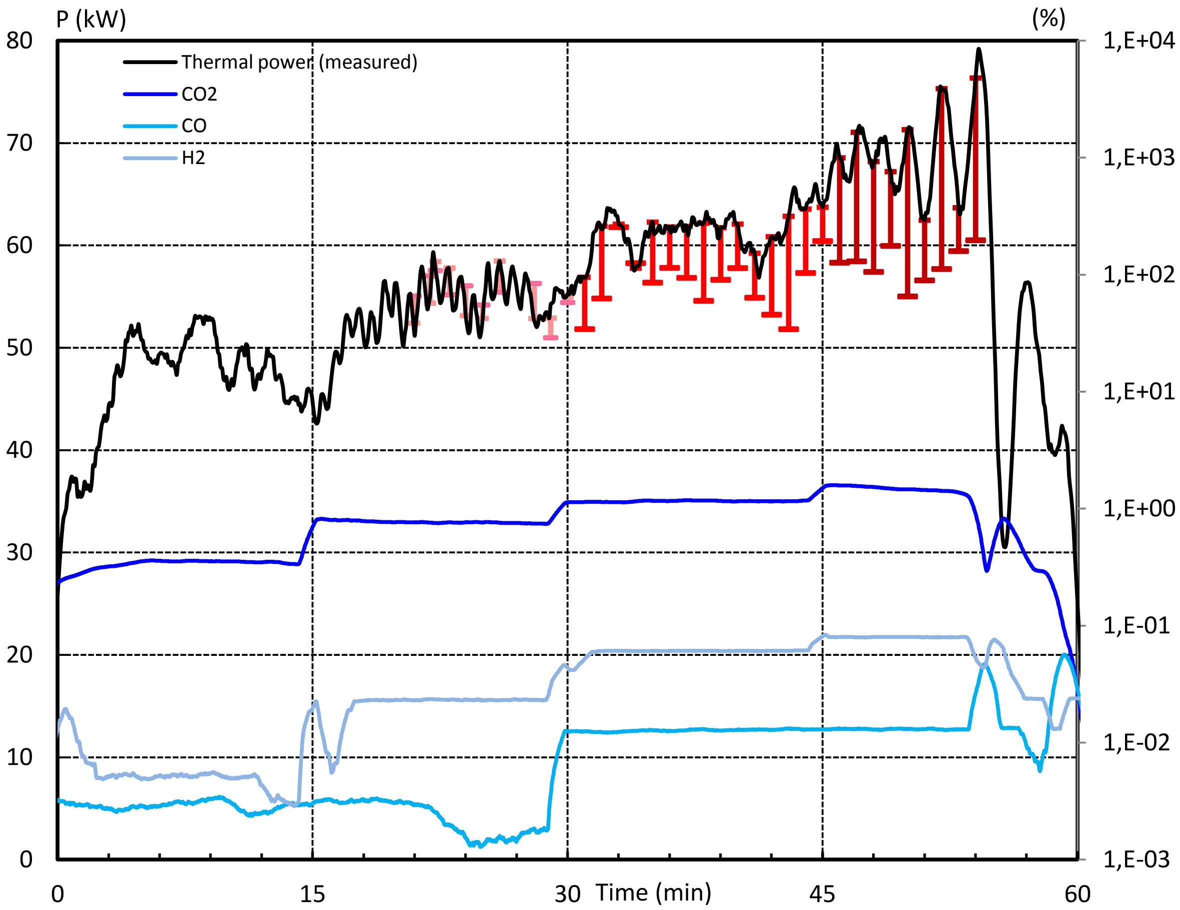

Figure 4: Total measured thermal power (black) , CO_2, CO and H_2 volume percentage (from dark to light blue). The colored arrows represent the difference between the total measured thermal power and the measured electric power at different biomass injection rate 1.1 $kg.h^{-1}$, 2.2 $kg.h^{-1}$ and 3.3 $kg.h^{-1}$ (from light to dark red).

Table 3: Summarized test results (CO_2, CO and H_2 emissions are in percentage of the total gas at the outlet which includes filter cooling flow. The total gas at the outlet is approximately 218 $Nm^3.h^{-1}$)

	Phase	Heating (without combustion)	Biomass feeding rate of 1.1 $kg.h^{-1}$	Biomass feeding rate of 2.2 $kg.h^{-1}$	Biomass feeding rate of 3.3 $kg.h^{-1}$	Average per kg
	Combustion power (kW)	--	5.28	5.49	6.11	5.62
NDIR	CO_2 emission (%)	0.355	0.403	0.416	0.415	0.411
NDIR	CO emission (%)	--	--	0.01	0.01	0.01
NDIR	H_2 emission (%)	0.005	0.023	0.038	0.019	0.026
CPG	CO_2 emission (%)	0,30	0,57	0.45	--	0.51
CPG	O_2 (%)	20,45	19,85	19,44	19,79	--
CPG	N_2 (%)	79,25	79,28	79,23	79,23	--

One of the advantages of this graphite electrode technology consists in considering the electrode as a consumable with the possibility of continuous feeding. Electrodes are consumed due to thermal erosion and chemical reaction with air. The high speed videos captured before the start of biomass injection, allowed the tracking of particles snatched from the graphite electrodes. In Figure 5, one of this particle is tracked between A and B during 20 ms, which gives a speed of 20 $m.s^{-1}$. Its trajectory is linear and is directly linked to the direction of the magnetic forces. During injection of the combustible, the biomass particles pass through the discharge zone, gain enough energy for surface vaporization and start combustion (Figure 6). The residence time cross the torch is equal to 7.5 ms which is relatively a short time when compared to coal thermal plant furnaces [13].

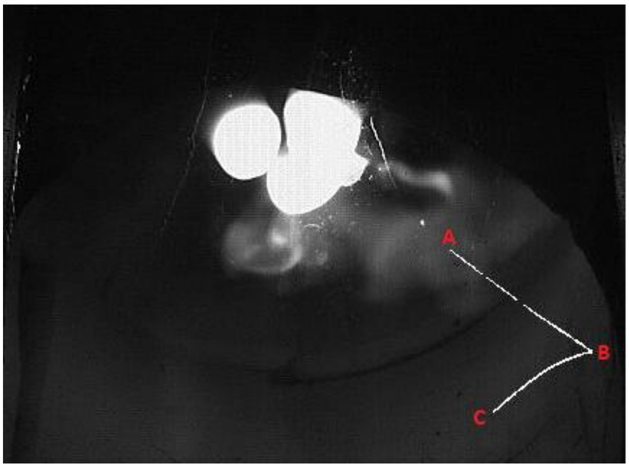

Figure 5: trajectory of a graphite electrode particle during a test without combustion (superposition of 300 frames captured at 150,000 fps)

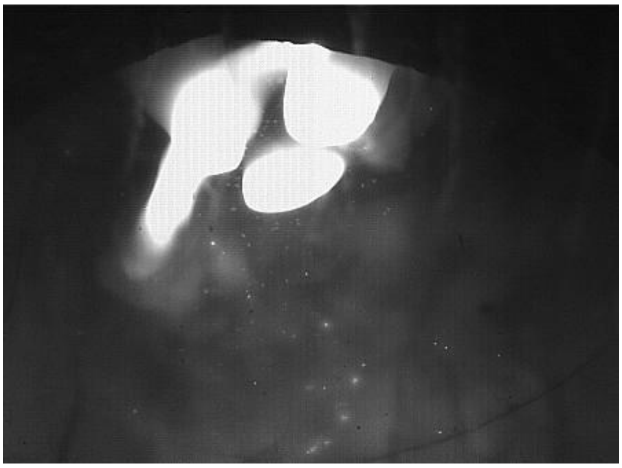

Figure 6: Shot of the arc discharge zone (electrode, electric arc and burning biomass particle) the feeding rate is 1 $kg.h^{-1}$.

4. Conclusion

The plasma assisted combustion tests described in this work are the first performed with this three phase graphite electrode plasma torch. The energy balance of wood ships combustion shows almost complete combustion for feeding rates from 1.1 to 3.3 $kg.h^{-1}$. according to NDIR and chromatography analysis of burned gases carbon monoxide production is negligible while CO_2 and H_2 emissions are consistent with power measurement and the feeding rate. Besides, high speed camera videos provided qualitative description of particle combustion during the crossing of the discharge zone and also the detachment of particle from the electrodes under the effect of mechanical erosion.

5. References

[1] Y. Ju, W. Sun, Combust. Flame 162 (2015) 529‑532
[2] J. M. Bergthorson, M. J. Thomson, Renew. Sustain. Energy Rev. 42 (2015) 1393‑1417
[3] S. S. Merola, L. Marchitto, C. Tornatore, G. Valentino, A. Irimescu, Appl. Therm. Eng. 69 (2014) 177‑187
[4] A. Starikovskiy, N. Aleksandrov, Prog. Energy Combust. Sci. 39 (2013) 61‑110
[5] A.-M. Warris, F. Weinberg, Symp. Int. Combust. 20 (1985) 1825‑1831

[6] M. Sijercic, S. Belosevic, P. Stefanovic, Therm. Sci. 9 (2005) 57‑72
[7] M. A. Gorokhovski, Z. Jankoski, F. C. Lockwood, E. I. Karpenko, V. E. Messerle, A. B. Ustimenko, Combust. Sci. Technol. 179 (2007) 2065‑2090
[8] A. V. Messerle, High Energy Chem. 38 (2004) 35‑40
[9] A. Askarova, E. . Karpenko, Y. . Lavrishcheva, V. E. Messerle, A. Ustimenko, IEEE Trans. Plasma Sci. 35 (2007) 1607‑1616
[10] A. D. Rychkov, M. F. Zhukov, J. Appl. Mech. Tech. Phys. 39 (1998) 441‑446
[11] C. Rehmet, V. Rohani, F. Cauneau, L. Fulcheri, Plasma Chem. Plasma Process. 33 (2013) 491‑515
[12] F. M. Zado, J. Fabecic, J. Chromatogr. A. 51 (1970) 37‑44
[13] H. Gao, A. J. Majeski, A. Runstedtler, Fuel. 108 (2013) 484‑489